

Benzoxazole-Based Heterometallic Dodecanuclear Complex $[\text{Dy}^{\text{III}}_4\text{Cu}^{\text{II}}_8]$ with Single-Molecule-Magnet BehaviorOlga Iasco,[†] Ghenadie Novitchi,^{†,‡} Erwann Jeanneau,[†] Wolfgang Wernsdorfer,[§] and Dominique Luneau^{*,†}[†]Laboratoire des Multimateriaux et Interfaces (UMR 5615), Université Claude Bernard Lyon 1, 69622 Villeurbanne Cedex, France[‡]Institute of Chemistry, Academy of Sciences of Moldova, Academiei, str. 3 MD-2028 Chisinau, Moldova[§]Institut Néel-CNRS, BP166, 25 Avenue des Martyrs, 38042 Grenoble Cedex 9, France

S Supporting Information

ABSTRACT: Three Cu–Ln (Ln = Dy, Gd, Y) dodecanuclear clusters assembled by a novel ligand of the benzoxazole type are reported. The dysprosium cluster exhibits a frequency dependence of the alternating-current susceptibility and hysteresis loop at low temperature, indicating single-molecule-magnet behavior.

Metal complexes, such as single-molecule magnets (SMMs), exhibiting versatile magnetic behavior have attracted special attention over the past decade.^{1,2} The origin of the SMM behavior is the easy-axis (Ising-type) magnetic anisotropy ($D < 0$), which causes the formation of an energy barrier to reorientation of the spin and can be defined in terms of a large-spin ground state and large magnetic anisotropy.²

In the search for SMMs, a special position has been attributed to 3d/4f heterometallic complexes where a high-spin ground state and strong magnetic anisotropy may result thanks to a favorable combination of magnetic interactions between the metal centers and the local magnetic anisotropy carried by lanthanide ions such as Dy^{III} and Tb^{III} .³ A number of such 3d/4f systems have been structurally and magnetically characterized. For example, see Cu/Ln,^{4–9} Ni/Ln,¹⁰ Co/Ln,¹¹ Fe/Ln,¹² Mn/Ln,¹³ and Cr/Ln.¹⁴ In this Communication, we report on the synthesis, structure, and magnetic properties of a new series of dodecanuclear molecular wheels, $[\text{Ln}^{\text{III}}_4\text{Cu}^{\text{II}}_8]$ [Ln = Dy (1), Gd (2), Y (3)], which were obtained using a ligand of the benzoxazole family.

The reaction of 3,5-di-*tert*-butyl-*o*-benzoquinone with ethanolamine, $\text{LnCl}_3 \cdot 6\text{H}_2\text{O}$, and $\text{CuCl}_2 \cdot 2\text{H}_2\text{O}$ at room temperature and under aerobic conditions in a 2:2:1:2 ratio in the presence of Et_3N leads to the formation of blue-turquoise needlelike crystals with the formula $[\text{Ln}_4\text{Cu}_8\text{L}_8(\mu_2\text{-H}_2\text{O})(\mu_3\text{-OH})_8\text{Cl}_{10}(\text{H}_2\text{O})_4]\text{Cl}_2 \cdot 6\text{MeCN}$ [Ln = Dy (1), Gd (2), Y (3); HL = 5,7-di-*tert*-butyl-2-methylenehydroxybenzoxazole; MeCN = acetonitrile]. The single-crystal X-ray diffraction data collected for all three compounds 1–3 show that they are isomorphic.

The crystal structure exemplified hereafter for $[\text{Dy}^{\text{III}}_4\text{Cu}^{\text{II}}_8]$ (1) consists of a complex cation $[\text{Dy}_4\text{Cu}_8\text{L}_8(\mu_2\text{-H}_2\text{O})(\mu_3\text{-OH})_8\text{Cl}_{10}(\text{H}_2\text{O})_4]^{2+}$ crystallizing with two chloride anions for charge balance and molecules of acetonitrile (Figure 1). The cationic entities comprise four Dy^{III} at the vertices of a rhombus and eight Cu^{II} located all around and outside the rhombus. The complete architecture is formed by four slightly distorted heteronuclear $\{\text{Cu}_2\text{Dy}_2\text{L}_2(\text{OH})_2\}$ cubane-like moieties sharing

the Dy^{III} ions in a rhombus fashion. The arrangement of the $\{\text{Dy}_2\text{Cu}_2\text{L}_2(\text{OH})_2\}$ moieties is reminiscent of those reported by us previously for a nonanuclear $[\text{Dy}_3\text{Cu}_6]$ but sharing the Dy^{III} in a triangular fashion.⁴ A lateral look at the cluster shows four Dy^{III} ions sandwiched between two squares, each made of four Cu^{II} centers, with $\text{Cu} \cdots \text{Cu}$ distances of 5.164, 6.505 Å and 5.623, 6.930 Å and $\text{Cu}—\text{Cu}—\text{Cu}$ angles of 89.40–90.60° (Figures 1 and S2 in the Supporting Information).

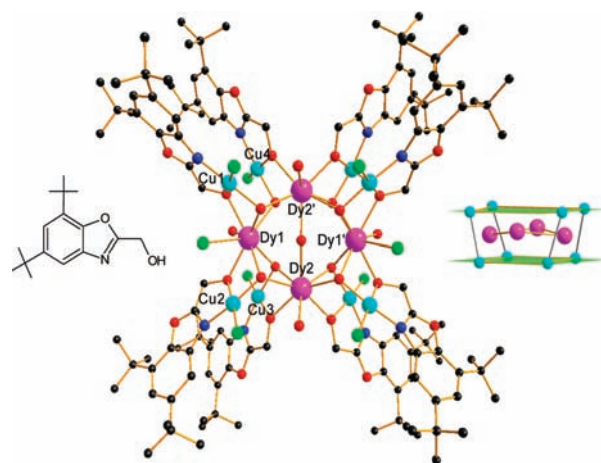


Figure 1. Structure of the cation $[\text{Dy}_4\text{Cu}_8\text{L}_8(\mu_2\text{-H}_2\text{O})(\mu_3\text{-OH})_8\text{Cl}_{10}(\text{H}_2\text{O})_4]^{2+}$ with scheme of the ligand and view of the Dy^{III} ions sandwiched between the Cu^{II} ions. The solvent molecules and hydrogen atoms are omitted for clarity.

Eight oxygens from the alkoxy groups of the deprotonated ligand L^- and eight oxygen atoms from the hydroxo groups bridge the Dy^{III} and Cu^{II} metal ions in a μ_3 fashion. Each alkoxy group connects one Cu^{II} center with one Dy^{III} ion, and each hydroxo group links two Dy^{III} ions to one Cu^{II} ion. One molecule of water is found in the center of the cluster located on a C_2 axis and bridging two symmetrically related Dy^{III} ions in a μ_2 fashion.

Each of the four Dy^{III} ions are eight-coordinate. Seven positions come from four bridging hydroxo groups, two alkoxy groups of the deprotonated ligand L^- , and one coordinated water molecule. The eighth position is occupied differently by a chloride ion for the Dy1 ions, while it is a bridging water molecule

Received: May 20, 2011

Published: July 12, 2011

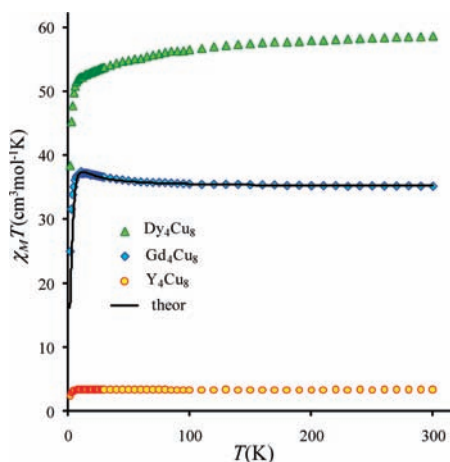


Figure 2. $\chi_M T$ vs T plot data for 1–3. The black solid lines correspond to the simulation according to the Hamiltonian with parameters described in the text.

for the Dy²⁺ ions (Figure S4 in the Supporting Information). Each of the Cu^{II} ions is coordinated in the plane by one nitrogen and one oxygen atom of a benzoxazole ligand {CuL} plus one hydroxo group and one chloride ion. The Cu–O, Cu–N, and Cu–Cl bond lengths are 1.921–2.020, 1.962–1.993, and 2.252–2.260 Å, respectively. An oxygen atom from a bridging alkoxo group belonging to the adjacent {CuL} unit is also found in the apical position. However, it is rather far at distances ranging from 2.304 to 2.923 Å. There are also two molecules of acetonitrile at 2.702 Å on the sixth position of Cu4 and Cu4'. These distances are also rather long. Thus, all Cu^{II} ions are viewed to have the same environment, which is best described as square-planar.

The temperature dependences of the magnetic susceptibility for 1–3 were measured on polycrystalline samples in the temperature range 2–300 K under an applied magnetic field of 0.1 T and are shown in Figure 2. The value of $\chi_M T$ (3.30 cm³·K·mol^{−1}) for 3 at room temperature is in good agreement with the calculated value of 3.308 cm³·K·mol^{−1} for eight Cu^{II} ions ($S = 1/2$ with $g = 2.10$). The variation of $\chi_M T$ with temperature is constant, as was expected for noninteracting Cu^{II} ions, in agreement with the presence of square-planar Cu^{II} in isolated {CuL} units. The decrease of $\chi_M T$ at low temperature (3 K) is most probably due to the effect of intermolecular interactions and/or weak Cu–Cu interactions.

The magnetization curves for 3 can be well fitted with a Brillouin function for eight Cu^{II} ions ($S = 1/2$ with $g = 2.10$) and is consistent with negligible values for the Cu–Cu interaction (Figure S5 in the Supporting Information).

The $\chi_M T$ value for 2 at room temperature is 35.15 cm³·K·mol^{−1} (Figure S6 in the Supporting Information) and agrees well with the expected value of 35.13 cm³·K·mol^{−1} for four Gd^{III} ions ($^8S_{7/2} = 7/2$ with $g = 2$) and eight Cu^{II} ions ($S = 1/2$ with $g = 2.10$) in accordance with the Cu^{II} values extracted from the corresponding yttrium analogue. Upon cooling, the $\chi_M T$ product increases to a maximum value of 37.11 cm³·K·mol^{−1} at 10 K and 0.1 T. Below 10 K, the $\chi_M T$ product sharply decreases and reaches the value of 25.04 cm³·K·mol^{−1} at 2 K. This behavior indicates the presence of both ferromagnetic and antiferromagnetic interactions. According to the X-ray diffraction investigation on single crystals, clusters 1–3 are isomorphous.

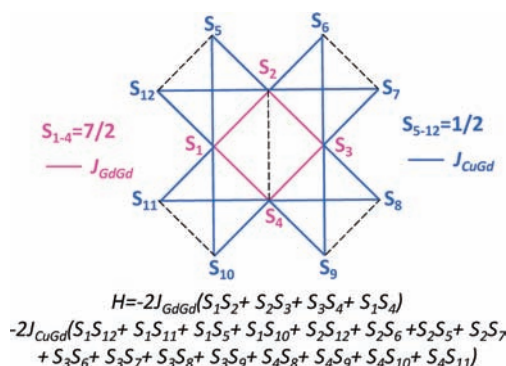


Figure 3. Spin topology and Hamiltonian for cluster 2 (Gd₄Cu₈).

Thus, as for compound 2, we can also neglect the Cu–Cu interaction and use the following isotropic spin Hamiltonian for simulation of the magnetic susceptibility for (Figure 3):¹⁵ where J_{GdGd} and the first term of the Hamiltonian address the magnetic interaction in the central Gd₄ core (rhomb) and J_{CuGd} and the second term hold for the magnetic interaction between Cu and Gd. Because of the similarity of the bridging functions for all Cu/Gd pairs and to avoid overparameterization, we used only one common parameter (J_{GdGd} and J_{CuGd}) for each of the Gd–Gd and Cu–Gd magnetic interactions (Figure 3). The estimated J values can be found by simulation of the $\chi_M T$ and magnetization curves using the indicated Hamiltonian.¹⁵ The best coincidence of the experimental and calculated values of the $\chi_M T$ product and magnetization is obtained for $J_{\text{GdGd}} = -0.15 \text{ cm}^{-1}$, $J_{\text{CuGd}} = +0.5 \text{ cm}^{-1}$, $zJ = -0.019 \text{ cm}^{-1}$, and $g = 2.10$ (see Figures 2 and S6 in the Supporting Information), which correspond, as may be expected, to a weak antiferromagnetic Gd–Gd magnetic interaction and a weak ferromagnetic Cu–Gd interaction.¹⁶

The product of $\chi_M T$ for compound 1 at $H = 0.1$ T decreases from 58.55 cm³·K·mol^{−1} at room temperature to 38.14 cm³·K·mol^{−1} at 2.0 K (Figure 2). The value at room temperature is close to the expected value of 59.99 cm³·K·mol^{−1} for four Dy^{III} ions ($^6H_{15/2}$, $L = 5$, and $g = 4/3$)¹⁷ and eight Cu^{II} ions ($S = 1/2$ with $g = 2.10$). The experimental values for the field dependence of magnetization at 2 and 5 K for 1 are typical and indicate the presence of anisotropy in compound 1 (Figure S7 in the Supporting Information). Alternating-current (ac) magnetic susceptibility measurements performed in a 2–12 K range using a 2.7 G ac field oscillation in a 1–1400 Hz frequency range for compound 1 are depicted in Figure S8 in the Supporting Information. The temperature dependence of the in-phase susceptibility shows frequency dependence but without maxima as a result of either a low-energy barrier of magnetic relaxation or tunneling. The application of a small direct-current (dc) field in the range 0.01–0.1 T does not change the ac signal profile, suggesting that the slow magnetic relaxation (at 2 K) is not influenced by tunneling effects. The presence of a slow magnetic relaxation for 1 suggests the SMM behavior.

To confirm the SMM behavior, the magnetization versus applied dc field data were collected on single crystals of 1 using a micro-SQUID apparatus at the 0.04–0.6 K range.¹⁸ This revealed hysteresis loops, whose coercivity was temperature- and sweep-rate-dependent, increasing upon cooling and with an increase in the field sweep rate, respectively, as was expected for the superparamagnetic-like behavior of an SMM (Figure 4 and Figure S9).

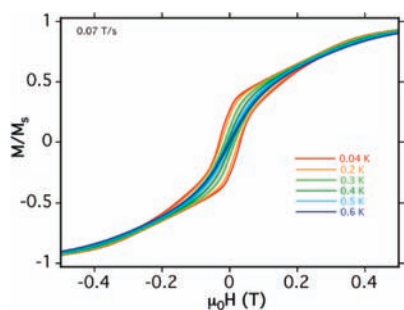


Figure 4. Plot of normalized magnetization (M/M_s) vs applied field (μ_0H) for **1** (Dy_4Cu_8). The loops are shown at different temperatures at $0.07 \text{ T} \cdot \text{s}^{-1}$.

The Dy_4 core in **1** is clearly responsible for this SMM behavior. The shape of the hysteresis loops and the cluster topology core is quite similar to that previously reported for a $[\text{Dy}_4\text{Cr}_4]$ system,¹⁴ suggesting that there is an analogous orientation of the main anisotropy axes in the central Dy_4 core.

In conclusion, a new series of dodecanuclear heterometallic $\text{Cu}^{\text{II}}/\text{Ln}^{\text{III}}$ [$\text{Ln} = \text{Dy}$ (**1**), Gd (**2**), Y (**3**)] clusters using benzoxazole-type ligands are reported. For **2**, magnetic data reveal the presence of ferromagnetic Cu–Gd and antiferromagnetic Gd–Gd interactions. The frequency dependence of the ac signals and magnetization hysteresis loop suggests that complex **1** is a new SMM.

■ ASSOCIATED CONTENT

S Supporting Information. Experimental procedure and crystallographic refinement details for **1–3**, the packing of clusters in the crystal lattice, and additional magnetic data. This material is available free of charge via the Internet at <http://pubs.acs.org>.

■ AUTHOR INFORMATION

Corresponding Author

*E-mail: luneau@univ-lyon1.fr.

■ ACKNOWLEDGMENT

O.I. acknowledges the French Ministry of Education for a Ph. D. grant, and G.N. thanks the Marie Curie Actions for funding during his stay at the Laboratoire des Multimatériaux et Interfaces. The authors thank Professor A. K. Powell for fruitful discussions. This work is partially supported by the ANR-PNANO project MolNanoSpin No. ANR-08-NANO-002, ERC Advanced Grant MolNanoSpin No. 226558, and STEP MolSpinQIP (to W.W.).

■ REFERENCES

- (1) (a) Gatteschi, D.; Sessoli, R. *Angew. Chem., Int. Ed.* **2003**, *42*, 268–297. (c) Wernsdorfer, W.; Sessoli, R. *Science* **1999**, *284*, 133–135.
- (b) Thomas, L.; Lionti, F.; Ballou, R.; Gatteschi, D.; Sessoli, R.; Barbara, B. *Nature* **1996**, *383*, 145–147.
- (2) Gatteschi, D.; Sessoli, R.; Villain, J. *Molecular Nanomagnets*; Oxford University Press: Oxford, U.K., 2006.
- (3) (a) Sessoli, R.; Powell, A. K. *Coord. Chem. Rev.* **2009**, *253*, 2328–2341. (b) Andruh, M.; Costes, J. P.; Diaz, C.; Gao, S. *Inorg. Chem.* **2009**, *48*, 3342–3359. (c) Sorace, L.; Benelli, C.; Gatteschi, D. *Chem. Soc. Rev.* **2011**, *40*, 3092–3104.

- (4) (a) Aronica, C.; Pilet, G.; Chastanet, G.; Wernsdorfer, W.; Jacquot, J. F.; Luneau, D. *Angew. Chem., Int. Ed.* **2006**, *45*, 4659–4662. (b) Aronica, C.; Chastanet, G.; Pilet, G.; Le Guennic, B.; Robert, V.; Wernsdorfer, W.; Luneau, D. *Inorg. Chem.* **2007**, *46*, 6108–6119.
- (5) (a) Novitchi, G.; Wernsdorfer, W.; Chibotaru, L. F.; Costes, J. P.; Anson, C. E.; Powell, A. K. *Angew. Chem., Int. Ed.* **2009**, *48*, 1614–1619. (b) Novitchi, G.; Costes, J. P.; Tuchagues, J. P.; Vendier, L.; Wernsdorfer, W. *New J. Chem.* **2008**, *32*, 197–200.
- (6) Baskar, V.; Gopal, K.; Helliwell, M.; Tuna, F.; Wernsdorfer, W.; Winpenny, R. E. P. *Dalton Trans.* **2010**, *39*, 4747–4750.
- (7) (a) Kajiwara, T.; Takahashi, K.; Hiraizumi, T.; Takaishi, S.; Yamashita, M. *CrystEngComm* **2009**, *11*, 2110–2116. (b) Kajiwara, T.; Nakano, M.; Takaishi, S.; Yamashita, M. *Inorg. Chem.* **2008**, *47*, 8604–8606.
- (8) (a) Okazawa, A.; Nogami, T.; Nojiri, H.; Ishida, T. *Chem. Mater.* **2008**, *20*, 3110–3119. (b) Okazawa, A.; Nogami, T.; Nojiri, H.; Ishida, T. *Inorg. Chem.* **2008**, *47*, 9763–9765. (c) Okazawa, A.; Nogami, T.; Nojiri, H.; Ishida, T. *Inorg. Chem.* **2009**, *48*, 3292–3292.
- (9) (a) Costes, J. P.; Dahan, F.; Wernsdorfer, W. *Inorg. Chem.* **2006**, *45*, 5–7. (b) Osa, S.; Kido, T.; Matsumoto, N.; Re, N.; Pochaba, A.; Mrozinski, J. J. *Am. Chem. Soc.* **2004**, *126*, 420–421. (c) Costes, J. P.; Vendier, L.; Wernsdorfer, W. *Dalton Trans.* **2010**, *39*, 4886–4892.
- (10) (a) Chandrasekhar, V.; Pandian, B. M.; Boomishankar, R.; Steiner, A.; Viftal, J. J.; Hourai, A.; Clerac, R. *Inorg. Chem.* **2008**, *47*, 4918–4929. (b) Dhers, S.; Sahoo, S.; Costes, J. P.; Duhayon, C.; Ramasesha, S.; Sutter, J. P. *CrystEngComm* **2009**, *11*, 2078–2083. (c) Sutter, J. P.; Dhers, S.; Rajamani, R.; Ramasesha, S.; Costes, J. P.; Duhayon, C.; Vendier, L. *Inorg. Chem.* **2009**, *48*, 5820–5828. (d) Pasatou, T. D.; Etienne, M.; Madalan, A. M.; Andruh, M.; Sessoli, R. *Dalton Trans.* **2010**, *39*, 4802–4808.
- (11) (a) Chandrasekhar, V.; Pandian, B. M.; Vittal, J. J.; Clerac, R. *Inorg. Chem.* **2009**, *48*, 1148–1157. (b) Costes, J. P.; Vendier, L.; Wernsdorfer, W. *Dalton Trans.* **2011**, *40*, 1700–1706. (c) Yamaguchi, T.; Costes, J. P.; Kishima, Y.; Kojima, M.; Sunatsuki, Y.; Brefuel, N.; Tuchagues, J. P.; Vendier, L.; Wernsdorfer, W. *Inorg. Chem.* **2010**, *49*, 9125–9135.
- (12) (a) Akhtar, M. N.; Mereacre, V.; Novitchi, G.; Tuchagues, J. P.; Anson, C. E.; Powell, A. K. *Chem.—Eur. J.* **2009**, *15*, 7278–7282. (b) Abbas, G.; Lan, Y.; Mereacre, V.; Wernsdorfer, W.; Clerac, R.; Buth, G.; Sougrati, M. T.; Grandjean, F.; Long, G. J.; Anson, C. E.; Powell, A. K. *Inorg. Chem.* **2009**, *48*, 9345–55. (c) Ferbinteanu, M.; Kajiwara, T.; Choi, K. Y.; Nojiri, H.; Nakamoto, A.; Kojima, N.; Cimpoesu, F.; Fujimura, Y.; Takaishi, S.; Yamashita, M. *J. Am. Chem. Soc.* **2006**, *128*, 9008–9009.
- (13) (a) Zaleski, C. M.; Kampf, J. W.; Mallah, T.; Kirk, M. L.; Pecoraro, V. L. *Inorg. Chem.* **2007**, *46*, 1954–1956. (b) Stamatatos, T. C.; Teat, S. J.; Wernsdorfer, W.; Christou, G. *Angew. Chem., Int. Ed.* **2009**, *48*, 521–524. (c) Mishra, A.; Tasiopoulos, A. J.; Wernsdorfer, W.; Moushi, E. E.; Moulton, B.; Zaworotko, M. J.; Abboud, K. A.; Christou, G. *Inorg. Chem.* **2008**, *47*, 4832–4843. (d) Zaleski, C. M.; Depperman, E. C.; Kampf, J. W.; Kirk, M. L.; Pecoraro, V. L. *Angew. Chem., Int. Ed.* **2004**, *43*, 3912–3914. (e) Mereacre, V.; Ako, A. M.; Clerac, R.; Wernsdorfer, W.; Hewitt, I. J.; Anson, C. E.; Powell, A. K. *Chem.—Eur. J.* **2008**, *14*, 3577–3584. (f) Mishra, A.; Wernsdorfer, W.; Parsons, S.; Christou, G.; Brechin, E. K. *Chem. Commun.* **2005**, 2086–2088.
- (14) Rinck, J.; Novitchi, G.; Van den Heuvel, W.; Ungur, L.; Lan, Y.; Wernsdorfer, W.; Anson, C. E.; Chibotaru, L. F.; Powell, A. K. *Angew. Chem., Int. Ed.* **2010**, *49*, 7583–7587.
- (15) Borrás-Almenar, J. J.; Clemente-Juan, J. M.; Coronado, E.; Tsukerblat, B. S. *J. Comput. Chem.* **2001**, *22*, 985–991.
- (16) (a) Rajaraman, G.; Totti, F.; Bencini, A.; Caneschi, A.; Sessoli, R.; Gatteschi, D. *Dalton Trans.* **2009**, 3153–3161. (b) Cirera, J.; Ruiz, E. C. R. *Chim.* **2008**, *11*, 1227–1234. (c) Costes, J. P.; Dahan, F.; Nicodeme, F. *Inorg. Chem.* **2001**, *40*, 5285–5287. (d) Novitchi, G.; Shova, S.; Costes, J. P.; Mamula, O.; Gdaniec, M. *Inorg. Chim. Acta* **2005**, *358*, 4437–4442.
- (17) Benelli, C.; Gatteschi, D. *Chem. Rev.* **2002**, *102*, 2369–2387.
- (18) Wernsdorfer, W. Classical and quantum magnetization reversal studied in nanometer-sized particles and clusters. *Advances in Chemical Physics*; Wiley: New York, 2001; Vol. 118, pp 99–190.